Biochemical Engineering Journal 21 (2004) 73–81

Biochemical Engineering Journal

www.elsevier.com/locate/bej

Modeling and simulation of airlift bioreactors

H. Znad [a,*], V. Báleš [a], J. Markoš [a], Y. Kawase [b]

[a] *Department of Chemical and Biochemical Engineering, Faculty of Chemical and Food Technology, Slovak University of Technology, Radlinského 9, 81237 Bratislava, Slovak Republic*

[b] *Department of applied Chemistry, Toyo University, Japan*

Received 30 December 2003; received in revised form 5 May 2004; accepted 14 May 2004

Abstract

A tanks-in-series model was applied for mathematical modeling of the unsteady state performance of a semi batch operation in a 10.5 dm^3 internal loop airlift bioreactor for the production of gluconic acid by fermentation. A set of first order differential equations for the material balances of micro-organism, substrate, product, and dissolved oxygen around the hypothetical well mixed stages in the riser and the downcomer was solved simultaneously using the Athena software package. The kinetic model used considers the effect of two substrates (glucose and dissolved oxygen) on the growth rate.

Both the effect of airflow rate and the height of the airlift bioreactor on the gluconic acid production were investigated. The model has been validated with experimental data. The model is simple enough to be used in design studies and it can be adapted to airlift system configurations and fermentation systems other than gluconic acid fermentation.

Keywords: Airlift bioreactor; Gluconic acid; Dissolved oxygen; Modeling; Bioreactors

1. Introduction

Most industrial bioreactors are still conventional stirred tanks. As alternatives to them, recently, airlift bioreactor designs have received increased attention. Due to their simple construction and less shear stress imposed on shear sensitive cells compared with stirred tanks, they have potential applications in biotechnology industries. However, an accurate description of the performance of airlift bioreactors is still difficult [1,2]. Mixing in airlift bioreactors is usually imperfect and mathematical models for airlift bioreactors cannot be described by neither perfect mixing (continuous stirred tank reactors: CSTR) nor plug flow (plug flow reactors: PFR) [3,4]. The mixing model used in most of the previous investigations dealing with airlift bioreactors is an axial dispersion model (ADM) [3–6]. It should be noted that the ADM could describe satisfactorily only mixing, which slightly deviates from the plug flow [7]. Furthermore, a set of differential equations and boundary conditions obtained for the axial dispersion model has to be solved by rather complicated numerical techniques. The extension of the ADM to more complicated mixing is very difficult. On the other hand, a tanks-in-series model used in this work is applicable to the whole mixing extents including perfect mixing and plug flow mixing. Moreover, the tanks-in-series model provides a set of first order differential equations, which can be solved using rather simple numerical techniques. In the tanks-in-series model, a modification of the model for micromixing or back mixing can be accomplished simply by introducing back flow b, as the ratio of the back flow rate to the net forward liquid flow rate, which does not cause difficulty in solving the equations.

Therefore, the tanks-in-series model utilizes two parameters, the number of tanks in series N and the back flow b, while the ADM contains only one parameter, the axial dispersion coefficient D_{ax}, which characterizes the deviations from ideal flow. The relationship between these two models, can be represented by [8],

$$\frac{1}{Pe} = \frac{b + (1/2)}{N} \tag{1}$$

If back flow is absent, i.e., $b = 0$, Eq. (1) changes to the well known relationship between the tanks-in-series model and the ADM where the equivalent number of tanks is given by $Pe/2$. Eq. (1) has another interesting feature; it shows that the overall back mixing process is the addition of perfect mixing within each stage and finite back mixing between each stage.

* Corresponding author. Tel.: +421 259325267; fax: +421 252496743.
E-mail address: znad71@yahoo.com (H. Znad).

1369-703X/$ – see front matter © 2004 Elsevier B.V. All rights reserved.
doi:10.1016/j.bej.2004.05.005

Nomenclature

A_b	cross-sectional area under the baffle (m^2)
A_d	cross-sectional area of the downcomer (m^2)
A_r	cross-sectional area of the riser (m^2)
b	back flow
C_l	dissolved oxygen concentration ($g\,dm^{-3}$)
C_l^*	equilibrium dissolved oxygen concentration ($g\,dm^{-3}$)
DO	dissolved oxygen
D_{ax}	axial dispersion coefficient ($m^2\,s^{-1}$)
D_r	riser diameter (m)
g	gravitational acceleration ($m\,s^{-1}$)
h_D	height of dispersion (m)
h_L	height of gas-free liquid (m)
h_r	height of the riser (m)
K_B	form friction loss coefficient for the bottom section
k_la	overall oxygen mass transfer coefficient (h^{-1})
K_O	Contois oxygen limitation constant
K_S	Contois saturation constant
M	number of stages in the riser
m_O	maintenance coefficient g substrate (g cells h)$^{-1}$
m_S	maintenance coefficient g substrate (g cells h)$^{-1}$
N	number of stages in the bioreactor
P	product concentration ($g\,dm^{-3}$)
P_G	power input due to gas (W)
Pe	Peclet number
Q_l	liquid flow rate ($dm^3\,min^{-1}$)
Q_G	gas flow rate ($dm^3\,min^{-1}$)
S	substrate concentration ($g\,dm^{-3}$)
t	time (h)
U_{gr}	superficial liquid velocity in the downcomer ($m\,s^{-1}$)
U_{lr}	superficial liquid velocity in the riser ($m\,s^{-1}$)
V_b	volume of the bottom section (dm^3)
V_d	volume of the downcomer section (dm^3)
V_L	working volume of the reactor (dm^3)
V_{lr}	linear liquid velocity in the riser ($m\,s^{-1}$)
V_{ld}	linear liquid velocity in the downcomer ($m\,s^{-1}$)
V_r	volume of the riser section (dm^3)
V_t	volume of the top section (dm^3)
X	biomass concentration ($g\,dm^{-3}$)
Y_{PO}	yield constant g product/g oxygen
Y_{PS}	yield constant g product/g glucose
Y_{XO}	yield constant g biomass/g oxygen
Y_{XS}	yield constant g biomass/g glucose

Greek letters

α	growth-associated product formation coefficient
β	non-growth-associated product formation coefficient (h^{-1})
γ	growth associated parameter in the Luedeking-Pirt-like equation for substrate uptake g substrate/g biomass
δ	parameter in the Luedeking-Pirt-like equation for oxygen uptake g oxygen/g biomass
λ	non-growth associated parameter in the Luedeking-Pirt-like equation for substrate uptake g substrate/g biomass h (h^{-1})
μ	specific growth rate (h^{-1})
μ_m	maximum specific growth rate (h^{-1})
ε_{gd}	gas hold up in the downcomer
ε_{gr}	gas hold up in the riser
ρ_L	liquid density ($g\,dm^{-3}$)
ϕ	parameter in the Luedeking-Pirt-like equation for g oxygen/g biomass h oxygen uptake (h^{-1})
Ψ	parameter in Eq. (31)

An axial dispersion model and a tanks-in-series model have been applied to describe mixing in bioreactors, Table 1. In spite of the applicability and flexibility of the tanks-in-series model, only few investigations concerning modeling have been published for simulation of fermentation systems including imperfect mixing in an airlift bioreactor.

Turner and Mills [15] pointed out that the tanks-in-series or mixing cell model is more realistic and advantageous compared with the ADM. Prokop et al. [9] and Erickson et al. [10] examined the performance of a multistage tower fermentor using a tanks-in-series model with back flow. In their studies, bubble column bioreactors were considered rather than airlift bioreactors. Furthermore oxygen mass transfer was not taken into account. Ho et al. [11], Andre et al. [12] and Pigache et al. [14] applied tank-in-series models to simulate oxygen transfer in airlift bioreactors. However, they did not discuss cultivation of microorganisms in the bioreactors. Kanai et al. [16], applied the tanks-in-series model with back flow to simulate the cultivation in airlift bioreactors and to discuss their steady state performance.

The assumption of steady state operation is very common in the analysis of airlift bioreactors. However, the models for the steady state yield no information, as how the steady state is attained. Little work has been carried out on unsteady state performance of airlift bioreactors.

In this study, a mathematical model based on a tanks-in-series model with back flow has been developed to simulate the fermentation of gluconic acid in airlift bioreactors under unsteady state.

2. Mathematical modeling for airlift bioreactors

The airlift bioreactor is composed of a column, which is divided into the region containing the gas liquid up flow (the riser) and the region containing the gas liquid down flow (the downcomer). The airlift bioreactors are usually classified into internal loop and external loop bioreactors according to the type of liquid recirculation.

Table 1
Simulation of tower type bioreactors

Authors	Reactor	Kinetic model	Operation	Mixing model
Prokop et al. [9]	Airlift	Oxygen transfer	Continuous	Tanks-in-series with back flow
Erickson et al. [10]	Bubble column	Monod	Continuous	Tanks-in-series with back flow
Ho et al. [11]	Airlift	Oxygen transfer	Continuous and batch	Tanks-in-series with back flow
Merchuk and Stein [5]	Airlift	Monod	Continuous	Axial dispersion
Adler et al. [6]	Airlift	Monod	Continuous	Axial dispersion
Luttman et al. [3]	Airlift	Monod	Batch	Axial dispersion
Andre et al. [12]	Airlift	Oxygen transfer	Continuous and batch	Tanks-in-series
Lavric and Muntean [13]	Airlift	Monod	Continuous	Axial dispersion
Pigache et al. [14]	Airlift	Oxygen transfer	Continuous	Tanks-in-series

In this simulation, the mixing characteristics are described by a tanks-in-series model. In the tanks-in-series model, the flow in the airlift bioreactor is considered as flow through a series of equal sized, well-mixed stirred stages or tanks and the parameter describing non-ideal flow is the number of stages. The mixing characteristics of the riser, downcomer, top and bottom sections in airlift bioreactors are different [17]. For example, in the computer simulation model of Merchuk and Stein [18], the mixing characteristics in the riser and the downcomer were postulated as plug flow and the head space was considered to be well mixed. An extension for the incorporation of micro-mixing effects into the model can be done by introducing back flow. The model is represented schematically in Fig. 1. The bottom section ($i = 1$) is treated as a well-mixed stage. The riser and the top sections ($i = 2, \ldots, M$) are described as tanks-in-series with back flow. Since the flow in the downcomer ($j = M + 1, \ldots, N$) is relatively well defined, the back flow in the downcomer is neglected.

At the top section, most of gas bubbles passing upward in the riser disengages and only the rest is entrained downward by liquid recirculation into the downcomer. On the other hand, the flow in the downcomer is almost single-phase and relatively well defined. Therefore, the backmixing in the downcomer is neglected. The riser, including the top and bottom sections, is divided into (M) hypothetical well mixed stages. In other words, ($M - 2$) stages with back flow are used to characterize mixing in the riser. Consequently, mixing in the downcomer is represented by ($N - M$) stages without back flow. The stages in the riser are numbered upwards

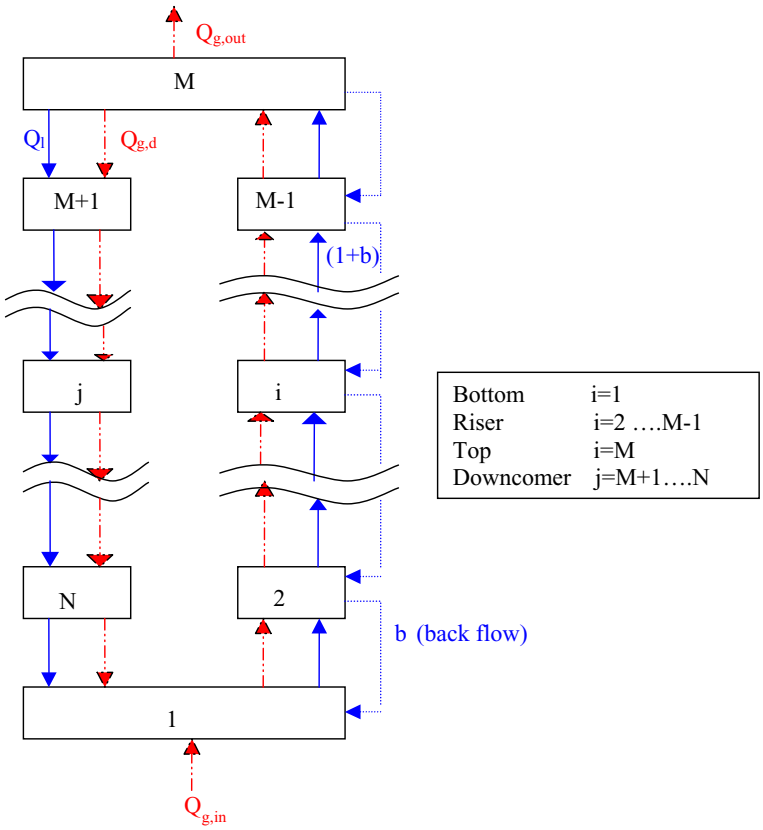

Fig. 1. Schematic diagram of the tank-in-series model for the airlift bioreactor.

and those in the downcomer are numbered downwards. The oxygen concentrations in the gas phase is assumed to be uniform [12], and the value of equilibrium dissolved oxygen concentration, C_l^*, was assumed constant throughout the fermentor and during the fermentation and equal to 0.00651 g dm^{-3}, i.e., $C_l(t = 0)$. At the bottom section, the gas feed and the recycle flow from the downcomer are introduced. It is assumed that the fermentation has a good temperature control and the temperature is constant. Consequently, in this study, energy balances are not taken into account, as well as in the work of Luttman et al. [3], and Kanai et al. [16].

2.1. Material balances in different sections of the ALR

The tanks-in-series model with back flow provides simultaneous first order ordinary differential equations, which are material balances of the microorganism, substrate, product, and dissolved oxygen for hypothetical well-mixed tanks or stages. The unsteady state material balances of these components can be written as follows:

2.1.1. Bottom section ($i = 1$)

For the micro-organism, substrate, and product ($C = X$, S, and P)

$$\frac{dC_l}{dt} = \frac{Q}{V_b(1-\varepsilon_{gr})}C_N + \frac{bQ}{V_b(1-\varepsilon_{gr})}C_2 - \frac{(1+b)Q}{V_b(1-\varepsilon_{gr})}C_1 + r_{C,1} \quad (2)$$

For the dissolved oxygen (C_l)

$$\frac{dC_{l,1}}{dt} = \frac{Q}{V_b(1-\varepsilon_{gr})}C_{l,N} + \frac{bQ}{V_b(1-\varepsilon_{gr})}C_{l,2} - \frac{(1+b)Q}{V_b(1-\varepsilon_{gr})}C_{l,1} + (k_l a)(C_{l,1}^* - C_{l,1}) + r_{o,1} \quad (3)$$

2.1.2. Riser section ($i = 2, \ldots, M-1$)

For the micro-organism, substrate, and product ($C = X$, S, and P).

$$\frac{dC_i}{dt} = \frac{bQ}{(V_r/(M-2))(1-\varepsilon_{gr})}[C_{i+1} - C_i] + \frac{(1+b)Q}{(V_r/(M-2))(1-\varepsilon_{gr})}[C_{i-1} - C_i] + r_{C,i} \quad (4)$$

For the dissolved oxygen (C_l)

$$\frac{dC_{l,i}}{dt} = \frac{bQ}{(V_r/(M-2))(1-\varepsilon_{gr})}[C_{l,i+1} - C_{l,i}] + \frac{(1+b)Q}{(V_r/(M-2))(1-\varepsilon_{gr})}[C_{l,i-1} - C_{l,i}] + k_l a(C_{l,i}^* - C_{l,i}) + r_{o,i} \quad (5)$$

2.1.3. Top section ($i = M$)

For the micro-organism, substrate, and product ($C = X$, S, and P)

$$\frac{dC_M}{dt} = \frac{Q(1+b)}{V_T(1-\varepsilon_{gr})}[C_{M-1} - C_M] + r_{C,M} \quad (6)$$

For the dissolved oxygen (C_l)

$$\frac{dC_{l,M}}{dt} = \frac{Q(1+b)}{V_T(1-\varepsilon_{gr})}[C_{l,M-1} - C_{l,M}] + k_l a(C_{l,M}^* - C_{l,M}) + r_{o,M} \quad (7)$$

2.1.4. Downcomer section ($i = M+1, \ldots, N$)

For the micro-organism, substrate, and product ($C = X$, S, and P)

$$\frac{dC_i}{dt} = \frac{Q}{(V_d/(N-M))(1-\varepsilon_{gd})}[C_{i-1} - C_i] + r_{C,i} \quad (8)$$

For the dissolved oxygen (C_l)

$$\frac{dC_{l,i}}{dt} = \frac{Q}{(V_d/(N-M))(1-\varepsilon_{gd})}[C_{l,i-1} - C_{l,i}] + k_l a(C_{l,i}^* - C_{l,i}) + r_{o,i} \quad (9)$$

where $r_{C,i} = r_{X,i}, r_{S,i}, r_{P,i}$

2.2. Kinetic model

The kinetic model presented in [19] will be used in this simulation to describe the gluconic acid fermentation. The model is given by Eqs. (10)–(14).

$$r_{X,i} = \frac{dX_i}{dt} = \mu_i X_i \quad (10)$$

$$r_{S,i} = \frac{dS_i}{dt} = -\gamma\frac{dX_i}{dt} - \lambda X_i \quad (11)$$

$$r_{P,i} = \frac{dP_i}{dt} = \alpha\frac{dX_i}{dt} + \beta X_i \quad (12)$$

$$r_{o,i} = \frac{dC_{l,i}}{dt} = -\delta\frac{dX_i}{dt} - \phi X_i \quad (13)$$

$i = 1 \rightarrow N$, where the specific growth rate (μ_i) is,

$$\mu_i = \mu_m \frac{S_i}{K_S X_i + S_i}\frac{C_{l,i}}{K_O X_i + C_{l,i}} \quad (14)$$

and

$$\gamma = \left(\frac{1}{Y_{XS}} + \frac{\alpha}{Y_{PS}}\right) \quad (15)$$

$$\lambda = \left(\frac{\beta}{Y_{PS}} + m_S\right) \quad (16)$$

$$\delta = \left(\frac{1}{Y_{XO}} + \frac{\alpha}{Y_{PO}}\right) \quad (17)$$

Table 2
Kinetic parameters estimated

Parameter	Kinetic parameters for 2 and 5 dm^3 STR [19]	Adjusted kinetic parameters for 10.5 dm^3 ALBR, this work
μ_m	0.3610	0.3610
α	2.580	4.5865
β	0.1704	1.3757
γ	2.1768	3.9868
λ	0.2937	0.9560
δ	0.2724	1.2699
ϕ	0.0425	0.0614
K_S	21.447	21.239
K_O	0.001061	0.004134

$$\phi = \left(\frac{\beta}{Y_{PO}} + m_O\right) \tag{18}$$

The specific growth rate defined by, Eq. (14), depends on two limiting substrates, i.e., glucose and dissolved oxygen. The kinetic parameters estimated from experiments in 2 and 5 dm^3 stirred tank reactors [19], have been used in the present simulation for predicting the gluconic acid fermentation in a 10.5 dm^3 airlift bioreactor. However, unfortunately, agreement between the simulation and experimental results was too poor. Therefore, adjusting of these kinetic parameters, is necessary to get a better agreement. The set of the adjusted kinetic parameters used in the simulations are summarized in Table 2. We believe that these parameters will be suitable for different airlift bioreactor scales.

2.3. Hydrodynamic and mass transfer correlations

The liquid velocities in the airlift bioreactor were calculated using the well known and widely tested model developed by Chisti for airlift devices [20],

$$U_{Lr} = \left[\frac{2gh_D(\varepsilon_{gr} - \varepsilon_{gd})}{K_B(A_r/A_d)^2(1/(1-\varepsilon_{gd})^2)}\right]^{0.5} \tag{19}$$

where

$$K_B = 11.40\left(\frac{A_d}{A_b}\right)^{0.79} \tag{20}$$

The height of the dispersion h_D was calculated from the known height h_L of the gas-free liquid and the overall gas holdup; thus,

$$h_D = \frac{h_L}{1-\varepsilon_g} \tag{21}$$

The superficial liquid velocity, Eq. (19), could be converted to the linear liquid velocity in the riser (V_{lr}) and the downcomer (V_{ld}),

$$V_{lr} = \frac{U_{Lr}}{1-\varepsilon_{gr}} \tag{22}$$

$$V_{lr}(1-\varepsilon_{gr})A_r = V_{ld}(1-\varepsilon_{gd})A_d \tag{23}$$

The gas hold-ups in the riser and the downcomer are related to the overall hold up by the analytical relations,

$$\varepsilon_g = \frac{A_r\varepsilon_{gr} + A_d\varepsilon_{gd}}{A_r + A_d} \tag{24}$$

The overall gas holdup was obtained by the following equation [20]:

$$\varepsilon_g = 4.334 \times 10^{-3}\left(\frac{P_G}{V_L}\right)^{0.499} \tag{25}$$

The following equation is necessary for calculation of ε_{gr} or ε_{gd},

$$\varepsilon_{gd} = 0.89\,\varepsilon_{gr} \tag{26}$$

For the axial dispersion coefficient of the liquid phase Towell and Ackermann [21], as cited in [22], found:

$$D_{ax} = 2.61 D_r^{1.5} U_{gr}^{0.5} \tag{27}$$

The overall oxygen transfer coefficient was calculated by the following equation [20],

$$k_la = 1.27 \times 10^{-4}\left(\frac{P_G}{V_L}\right)^{0.925} \tag{28}$$

where

$$\left(\frac{P_G}{V_L}\right) = \frac{\rho_L g U_{gr}}{1 + (A_d/A_r)} \tag{29}$$

$(k_la)_r$ and $(k_la)_d$ values were selected in such a way that the following two equations were satisfied:

$$k_la = \frac{(k_la)_r A_r + (k_la)_d A_d}{A_r + A_d} \tag{30}$$

$$(k_la)_d = \Psi(k_la)_r \tag{31}$$

The value of Ψ was fixed at 0.8 as recommended by Chisti [20]

3. Experiments

An internal-loop airlift bioreactor made of glass with a working volume of 10.5 dm^3 was used. The details of the bioreactor geometry are given in Table 3. The

Table 3
Basic parameter of the airlift reactor [22]

V_L (dm^3)	D (m)	h_L (m)	h_r (m)	D_r (m)	A_d/A_r	h_L/D	V_r (dm^3)	V_d (dm^3)	V_t (dm^3)	V_b (dm^3)
10.5	0.108	1.24	1.145	0.070	1.23	11.5	4.404	5.417	0.554	0.125

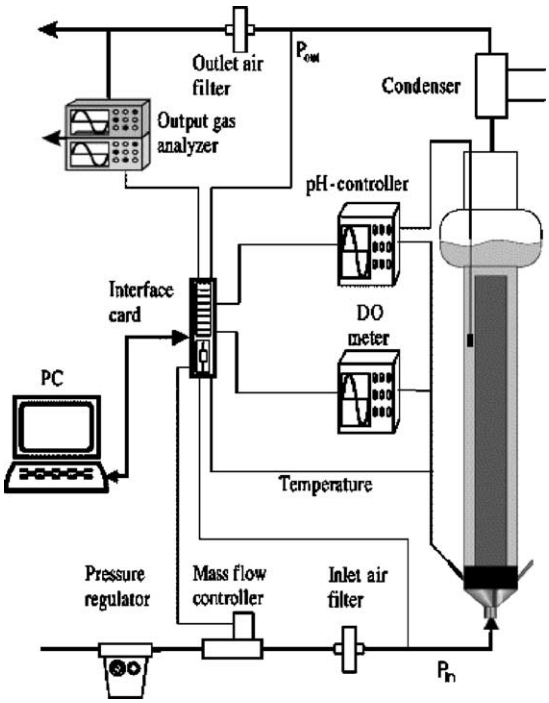

Fig. 2. Schematic diagram of the experimental apparatus [23].

scheme of the experimental equipment is depicted in Fig. 2 [23].

The microorganism *A. niger* CCM 8004 was used in this study. The mycelium grew in a pellet form. The inoculum was prepared in a shake flask for 48 h. The bioreactor was inoculated with 2% of volume. The reactor temperature was kept at 30 °C. Air was used as the gas phase. The airflow rate of 15 $dm^3\,min^{-1}$ (at 298 K and atmospheric pressure) was applied. Concentrations of gluconic acid and glucose in the sample solution were analyzed using high performance liquid chromatography (HPLC) [23].

4. Results and discussion

4.1. Determination of the model parameters

The values of gas-hold ups, mass transfer coefficients, and liquid circulation rate in an internal loop airlift bioreactor are required for computer simulations. These values can be evaluated using Eqs. (19)–(31) for our experimental conditions. The obtained results are given in Table 4. In this study, the gas hold up is assumed to be constant within both the downcomer and the riser sections. The value of the gas hold up in the head region (separator) is difficult to measure owing to the turbulent, wavy liquid surface; however, its value is assumed to be equal to that in the riser.

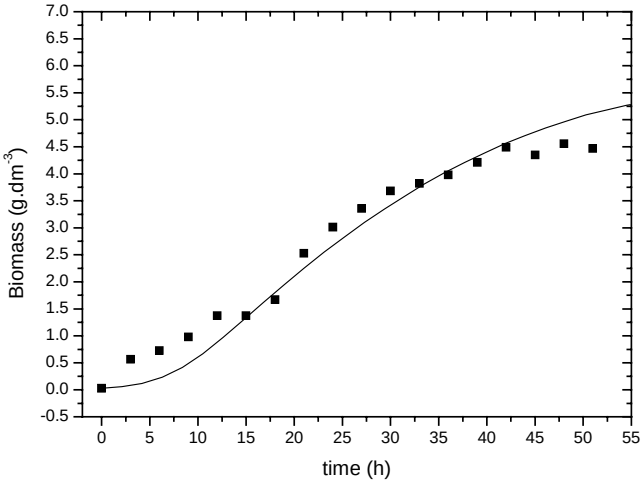

Fig. 3. Comparison of simulated (solid line) and experimental (points) profile of the biomass.

4.2. Estimation the number of stages in the riser and the downcomer

The extent of longitudinal mixing in the downcomer is represented by 10 stages ($N - M = 10$) or approximated as a plug flow [24]. To specify the number of stages in the riser including the top and bottom stages, i.e., M, Eq. (1) has been employed, as explained in Table 5.

The 7 stages in the riser are numbered 2–8 upwards, the 10 stages in the downcomer are numbered 10–19 downward, and the first and ninth stages represent the bottom and top sections, respectively, of the airlift bioreactor.

4.3. Simulation of gluconic acid production

Figs. 3–6, show typical time profiles of the biomass, gluconic acid, substrate, and dissolved oxygen, respectively, at an air flow rate of 15 $dm^3\,min^{-1}$ in a 10.5 dm^3 internal loop airlift bioreactor. During the exponential growth phase, the biomass concentration exponentially increases with cultivation time and the corresponding substrate concentration rapidly approaches zero. Growth rate decelerates due to depletion of the substrate and dissolved oxygen near the end of the exponential growth phase.

Moreover, these figures show the comparison of the simulated and experimental profiles for the biomass, gluconic

Table 4
Numerical values of the parameters used in the model

Q_l ($m^3\,s^{-1}$)	Q_g ($m^3\,s^{-1}$)	ε_{gr}	ε_{gd}	$(k_la)_r$ (s^{-1})	$(k_la)_d$ (s^{-1})	V_{lr} ($m\,s^{-1}$)	V_{ld} ($m\,s^{-1}$)
5.865×10^{-4}	2.566×10^{-4}	0.0785	0.0699	0.0273	0.0219	0.1655	0.133

Table 5
Evaluation of the number of stages in the riser (M)

h_D (m) Eq. (8)	$U_{gr} = Q_g/A_r$ (m s^{-1})	$D_{ax,r}$ (m^2 s^{-1}) Eq. (13)	$P_{e,r} = V_{lr}h_D/D_{ax,r}$	M, with $b = 0$ Eq. (1)
1.339	0.0667	0.0125	17.744	≈9

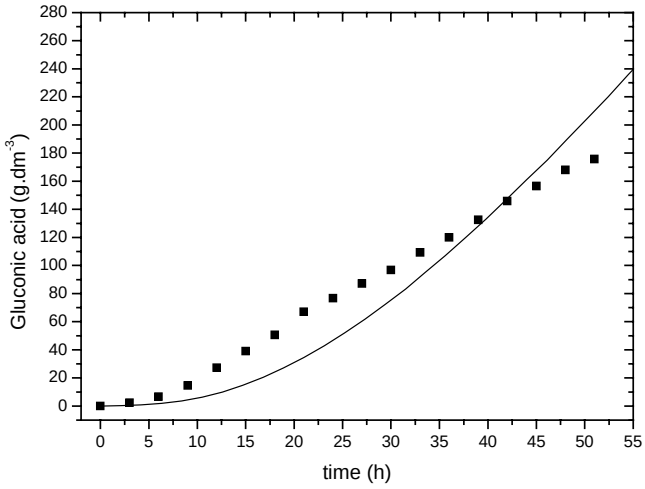

Fig. 4. Comparison of simulated (solid line) and experimental (points) profile of the GA.

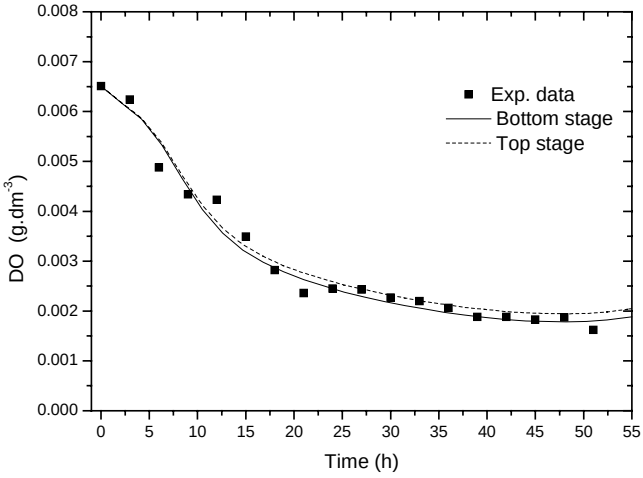

Fig. 6. Comparison of simulated (solid line) and experimental (points) profile of DO conc. at the first stage (solid line) and at the top (ninth) stage (dashed line) of the airlift bioreactor.

acid, substrate, and dissolved oxygen, respectively. The prediction of the model is quite good and it can finely describe the gluconic acid ferment in an airlift bioreactor.

4.4. Effect of air flow rate on the cell growth

Figs. 7 and 8, show the effect of airflow rate on the biomass growth and GA, keeping 57 h as a fixed time for the duration of fermentation. The biomass growth increased with increased airflow rate in the range of from 9 to 60 dm^3 min^{-1}. At aeration rate of 9 dm^3 min^{-1}, 3.55 g·dm^{-3} of biomass and 158 g·dm^{-3} of GA were produced in the scheduled time. The production of biomass and GA increased with the aeration rate and was stabilized at 6.21 g·dm^{-3} and 248 g·dm^{-3}, respectively, at an airflow rate of 45 dm^3 min^{-1}. Beyond 45 dm^3 min^{-1} the effect of airflow rate on the biomass growth and GA produced was not significant. This can be attributed to the fact that high airflow rates can lead to high gas hold ups, enhanced bulk mixing and improved DO and mass transfer, which promotes the biomass growth and consequently the gluconic acid. When the airflow rate exceeded 45 dm^3 min^{-1}, the increase in the biomass growth with airflow rate was reduced. The reason of this was that because high airflow rate

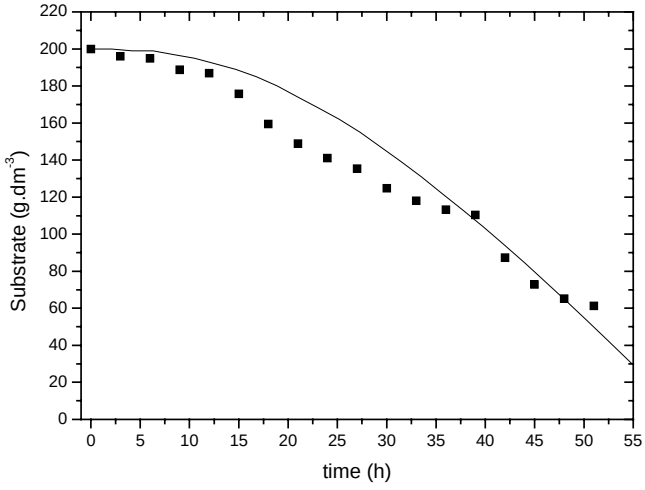

Fig. 5. Comparison of simulated (solid line) and experimental (points) profile of the substrate.

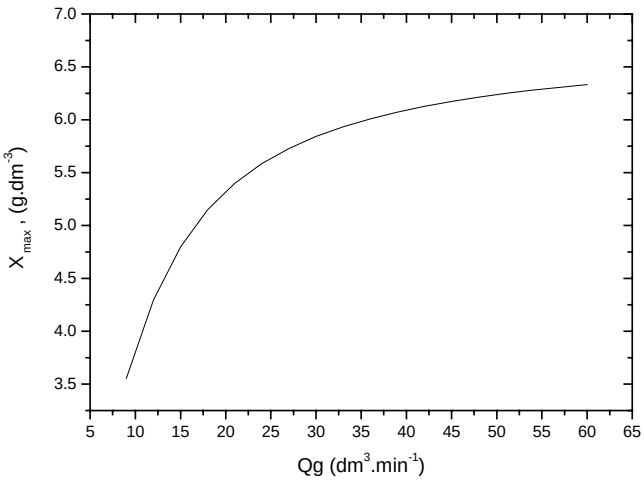

Fig. 7. Effect of air flow rate on the biomass concentration at 57 h of fermentation.

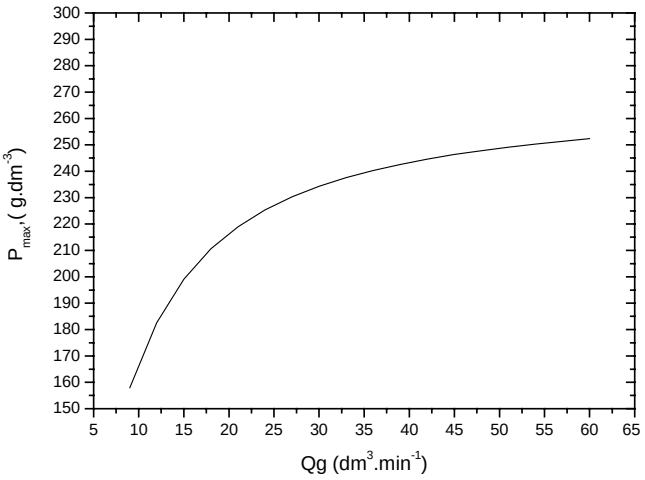

Fig. 8. Effect of air flow rate on the gluconic acid at 57 h of fermentation.

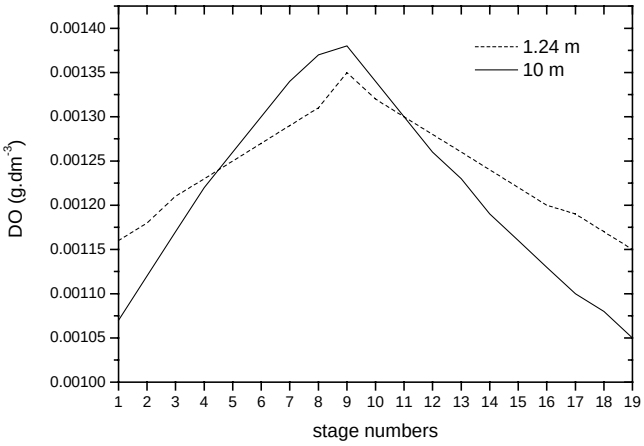

Fig. 10. Axial variation of DO concentration in 1.24 m (dashed line) and 10 m (solid line) airlift bioreactor at $Q_g = 15\,dm^3\,min^{-1}$ after 65 h of fermentation.

produced a high shear stress, which could potentially lead to cellular damage, consequently reducing the ability of cells to produce gluconic acid. Another reason could be, that higher airflow rates resulted in higher respiration rates, potentially leading to a significant decrease in glucose source (substrate) availability for any purpose, including gluconic acid synthesis, Fig. 9. The results show that there was an optimum range of airflow rate from 9 to 45 $dm^3\,min^{-1}$ for gluconic acid fermentation in a 10.5 dm^3 internal loop airlift bioreactor. This would have an additional process benefit of minimizing the costs of compressed air, a major contributor to the cost of running a large-scale airlift bioreactor [20].

4.5. Axial dissolved oxygen profile

Fig. 10 shows that the dissolved oxygen profile in the riser (2–8 stages) ascends because air is supplied in the riser and gas–liquid mass transfer occurs. In the riser, the interfacial mass transfer rate may be larger than the oxygen consumption of microorganisms and therefore, dissolved oxygen concentrations increased along the riser. However, the dissolved oxygen profiles descend in the downcomer (10–19 stages), in which no gas dispersion occurs and the consumption of microorganisms is higher than the mass transfer rate. Consequently, in the downcomer, oxygen is significantly consumed and as a result the dissolved oxygen concentration in the downcomer decreases significantly.

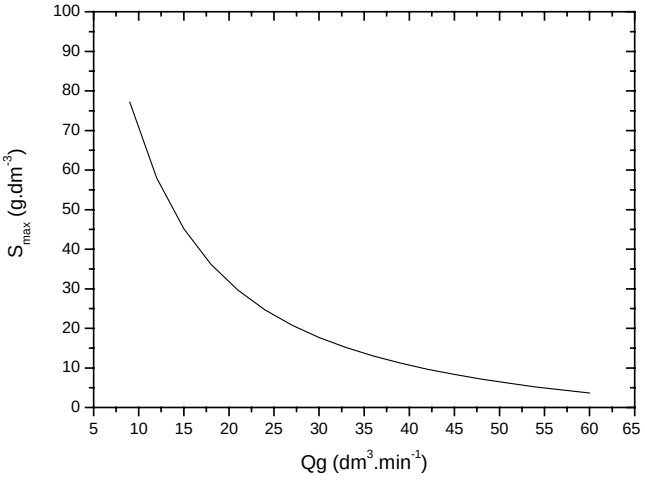

Fig. 9. Effect of air flow rate on the substrate at 57 h of fermentation.

To show the effect of the bioreactor height on the axial dissolved oxygen concentrations, two airlift bioreactors have been considered, a short one (1.24 m) and a tall hypothetical one (10 m), assuming constant gas flow rate and constant cross-sectional areas for both of the bioreactors. The result was illustrated in Fig. 10. The shorter reactor (dashed line) has, a relatively more uniform DO concentration than the taller one (solid line), where the change of DO concentration in the riser and the downcomer for the airlift bioreactor of 1.24 m height is 1.9×10^{-4} and 2×10^{-4}, respectively. For the airlift bioreactor of 10 m height these values are 3.1×10^{-4} and 3.3×10^{-4}, respectively. The DO concentration in the 10 m airlift bioreactor is higher because of the greater oxygen partial pressure caused by the liquid head. Furthermore, in the taller airlift bioreactor, the mean bubble residence time is longer and a larger fraction of oxygen is absorbed by the liquid phase. Because of these factors, the DO concentration at the bottom of the riser (stage 1) and the downcomer (stage 19) is lower in the 10 m-airlift bioreactor than that in the 1.24 m bioreactor. The results of simulation showed that the lowest levels of DO occur at the base of the bioreactor. This is in agreement with Hatch's experimental measurements [25] and theoretical observation of Ho et al. [11].

Fig. 11 shows the variation of the dissolved oxygen concentration with time and the number of the stages. At the beginning of fermentation the DO concentration is constant along the bioreactor. However, during the course of fermentation the concentration will change as presented in Fig. 10.

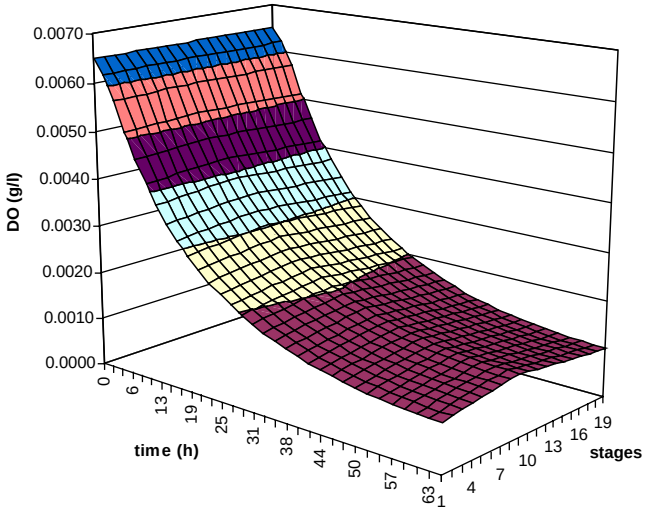

Fig. 11. DO concentrations profile along the airlift bioreactor under unsteady state conditions.

5. Conclusions

In this study, a mathematical model using tanks-in-series under unsteady state conditions is developed to describe the production of gluconic acid in an airlift bioreactor. The model has been tested and the values were compared with experimental data.

The model is suitable to predict the effect of airflow rate on the process. For gluconic acid fermentation an optimum range of airflow rate (9–45 $dm^3\,min^{-1}$) is suitable in a 10.5 dm^3 internal loop airlift bioreactor beyond which the process will not be economical. Also the effect of the bioreactor height on the axial dissolved oxygen has been predicted by the model. The shorter bioreactor, shows relatively more uniform axial DO concentrations than the longer bioreactor, where a greater variation in DO concentrations with the height was observed.

For further improvement of the model accuracy, more suitable correlations for the mass transfer coefficient and gas hold ups in a real fermentation system should be taken into account in the model.

Acknowledgements

This work was supported by the Slovak Grant Agency for Science VEGA (Grant No. 1/0066/03).

References

[1] U. Onken, P. Weiland, Airlift Fermenters: Construction, Behavior, and Uses, Advances in Biotechnological Processes, vol. 1, Alan R. Liss, New York, 1983.
[2] J.C. Merchuk, in: K. Scuger (Ed.), Biotechnology, second ed., VCH, Weinheim, 1993.
[3] R. Luttman, M. Thoma, H. Buchholz, K. Schugerl, Model development, parameter identification, and simulation of SCP production processes in air lift tower reactor with external loop-I, Comput. Chem. Eng. 7 (1983) 43–50.
[4] R. Luttman, M. Thoma, H. Buchholz, K. Schugerl, Model development, parameter identification, and simulation of SCP production processes in air lift tower reactor with external loop-II, Comput. Chem. Eng. 7 (1983) 51–63.
[5] J.C. Merchuk, Y. Stein, R.I. Mateles, Distributed parameter model of an airlift fermentor, Biotechnol. Bioeng. 22 (1980) 1189–1211.
[6] I. Adler, W.D. Deckwer, K. Schugerl, Performance of tower loop bioreactors—II. Model calculations for substrate limited growth, Chem. Eng. Sci. 37 (1982) 417–424.
[7] C.Y. Wen, L.T. Fan, Models for Flow Systems and Chemical Reactors, Marcel Dekker, New York, 1975.
[8] J. Todt, J. Lucke, K. Schugerl, A. Renken, Gas holdup and longitudinal dispersion in different types of multiphase reactor and their possible application for microbial processes, Chem. Eng. Sci. 32 (1977) 369–375.
[9] A. Prokop, L.E. Erickson, J. Fernandez, A.E. Humphrey, Design and physical characteristics of a multistage, continuous tower, Biotechnol. Bioeng. 11 (1969) 945–966.
[10] L.E. Erickson, S.S. Lee, L.T. Fan, Modelling and analysis of tower fermentation processes. I. Steady state performance, J. Appl. Chem. Biotechnol. 22 (1972) 199–214.
[11] C.S. Ho, L.E. Erickson, L.T. Fan, Modeling and simulation of oxygen transfer in airlift fermentors, Biotechnol. Bioeng. 14 (1977) 1503–1522.
[12] G. Andre, C.W. Robinson, M. Moo-Young, New criteria for application of the well-mixed model to gas–liquid mass transfer studies, Chem. Eng. Sci. 38 (1983) 1845–1854.
[13] V. Lavric, O. Muntean, Revista de Chemie 38 (1987) 807–814.
[14] S. Pigache, G. Trystram, P. Dhoms, Oxygen transfer modeling and simulation for an industrial continuous airlift fermentor, Biotechnol. Bioeng. 39 (1992) 923–931.
[15] J.R. Turner, P.L. Mills, Comparison of axial dispersion and mixing cell models for design and simulation of Fischer–Tropsch slurry bubble column reactors, Chem. Eng. Sci. 45 (1990) 2317–2324.
[16] T. Kanai, T. Uzumaki, Y. Kawase, Simulation of airlift bioreactors: steady-state performance of continuous culture processes, Comput. Chem. Eng. 20 (1996) 1089–1099.
[17] P. Verlaan, A.M.M. van Eijs, J. Tramper, K. van't Riet, K.Ch.A.M. Luyben, Estimation of axial dispersion in individual sections of an airlift-loop reactor, Chem. Eng. Sci. 44 (1989) 1139–1146.
[18] J.C. Merchuk, Y. Stein, A distributed parameter model for airlift fermentor. Effects of pressure, Biotechnol. Bioeng. 23 (1981) 1309–1324.
[19] H. Znad, M. Blažej, V. Báleš, J. Markoš:, A kinetic model for gluconic acid production by *Aspergillus niger*, Chem. Pap. 58 (2004) 23–28.
[20] Y. Chisti, Airlift Bioreactors, Elsevier, London, 1989.
[21] G.D. Towell, G.H. Ackerman, in: Proceedings of the 5th European, 2nd International Symposium Chemical Reat. Engineering, Amsterdam, B3, 1972, pp. 1–13.
[22] A. Lubbert, S. Godo, Bubble column & airlift loop bioreactor, in: P. Kieran, M. Berovič (Eds.), Bioprocess Engineering Course Notes, The European Federation of Biotechnology, Supetra, Island of Brač, Croatia, 8–14 September 2001, pp. 151–167.
[23] M. Krošlák, Modeling of the fermentation in the airlift reactors, M.Sc thesis, Slovak University of Technology, Bratislava, 2000.
[24] A. Prokop, L.E. Erickson, J. Fernandez, A.E. Humphrey, Design and physical characteristics of a multistage, continuous tower fermentor, Biotechnol. Bioeng. 11 (1969) 945–966.
[25] R.T. Hatch, Experimental and theoretical studies of oxygen transfer in the airlift fermentor, Ph.D. thesis, MIT, 1973.